In silico Evaluation of Wearable Cardiac Defibrillator: Personalized Therapy Planning to Prevent Sudden Cardiac Death

Oishee Mazumder
TCS Research
Tata Consultancy Services
Kolkata, India
oishee.mazumder@tcs.com

Aniruddha Sinha
TCS Research
Tata Consultancy Services
Kolkata, India
aniruddha.s@tcs.com

***Abstract*—In this paper, we propose a computational model to predict and optimize the defibrillation mechanism of Wearable Cardiac Defibrillator (WCD). The computational model is developed from high resolution torso cardiac MRI followed by biophysical simulation to assess the efficacy of defibrillation by determining defibrillation thresholds (DFT) and extent of myocardial damage. A measure for quantifying such efficacy is proposed by calculating the divergence in the distribution of myocardial potential gradient obtained in silico, with respect to an ideal probabilistic distribution, defined for defibrillator success. Variations in defibrillation efficacy is simulated for using different shocking electrode configurations to assess the best defibrillator outcome with minimal myocardial damage. The developed model can be used for designing personalized WCD vests depending on subject specific anatomy and pathology.**

***Index Terms*—Defibrillator, Finite Element model, Weighted Kullback Leibler divergence, MRI, Myocardial damage.**

I. Introduction

Sudden cardiac death (SCD) is an unpredictable event causing around 13% of deaths in overall population worldwide and about 36% of deaths in heart failure patients [1]. Leading cause of SCD is attributed to ventricular arrhythmia (VA), ventricular fibrillation (VF) associated with acute myocardial ischemia. VF is usually lethal within minutes of its inception and if not immediately treated, leads to cardiac arrest [2]. Electrical defibrillation is the only effective therapy for cardiac arrest caused by ventricular fibrillation (VF) [3].

Due to the prompt action requirement in VF leading to SCD, implantable cardioverter defibrillator (ICD) is the popular choice for treatment of SCD. Medical literature suggests that prompt defibrillation after onset of VF episodes increases the survival rates to as high as 75%, whereas each minute of delay in defibrillation declines the chance of a favourable outcome by 10% [4].

Risk of SCD is usually predicted based on left ventricular ejection fraction (LVEF). For patients recovering from myocardial infraction or newly diagnosed heart failure, LVEF may improve with treatment and even though SCD is a possibility, ICD implantation may not be the best treatment plan. Being an invasive process along with the cost and its effect on quality of life, ICD implantation requires a rigorous patient evaluation and is only recommended when absolutely required. WCD is usually recommended to patients awaiting ICD, patients with ventricular assist device awaiting heart transplantation or in recovery phase after nonischemic cardiomyopathy [5]. WCD requires no surgical intervention, completely removable and has been shown to be equally efficient in terminating VA by defibrillation shocks [6].

Irrespective of the type of defibrillator, strong shocks required during defibrillation have serious adverse effects on myocardium property like change in contractility, mechanical dysfunction affecting hemodynamics [7]- [8] along with the possibility of ectopic excitation after depolarization initiating post shock arrhythmia. Hence, it is extremely important to tune and optimize the shock energy to get the desired effect [9]. Computational model analyzing defibrillation mechanism and the aftereffect of shock voltage in myocardium provides indepth understanding and helps in optimizing the defibrillation threshold [10]. Distribution of electric field in the heart is closely related to the nature of defibrillation. Defibrillation shock should be able to depolarize the heart homogeneously, without initiating reentry of wavefronts [11]. Mathematical modeling and computer simulation can predict the defibrillation effect and help in ICD standardization [12]. Computational cardiac models incorporate the concept of volume conduction and bidomain propagation in cardiac tissues to study the effect of defibrillation in both spatial and temporal domain. These models are computationally extensive and challenging with both time and memory constraints [13]. A rather simple, globally accepted index of defibrillation success is via determining Defibrillation threshold (DFT), which is derived from the critical mass hypothesis [14]. Finite Element (FE) models of defibrillation has been reported for ICD (both transverse and subcutaneous) along with electrode size optimization for varying patient size using DFT index [15]. However, there are no reported computational model to assess the defibrillation quality and effectiveness of WCD with respect to electrode configuration, voltage, and energy requirement, for minimal myocardial damage.

In this paper, we propose a cardiac computational model for in silico defibrillation evaluation and optimization in terms of electrode configuration for WCD. Key contributions include developing a FE pipeline for WCD evaluation and proposing a new evaluation measure combining DFT and myocardial damage probability, which would aid in configuring probable shock electrode configurations for WCD performance optimization. The pipeline for subject specific image based FE modeling and evaluation would help in creating personalized WCD settings to reach DFT at a minimum myocardial damage configuration. This would result in optimum shock deliver configuration for specific subject anatomy, enabling a personalized therapy approach.

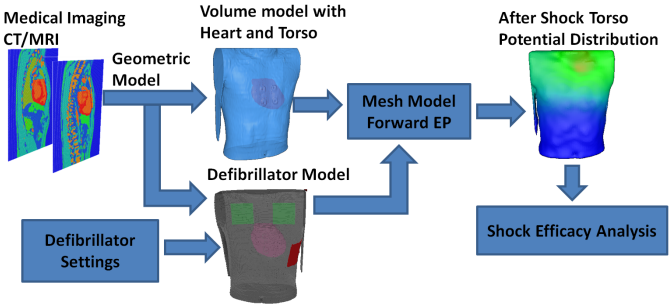

Fig. 1: Schematic of the proposed model

II. Methodology

Proposed pipeline for evaluating WCD performance starts with creating a 3D volume from torso-cardiac MRI slices. FE meshes are created in the torso to help in solving the biophysical model associated with application of external fibrillation. This is similar to 'Forward electrophysiology', only difference being that instead of using cardiac potential as the source model, defibrillator voltage is acting as the source. We use monodomain equations to solve the biophysical model. From the torso cardiac geometry, electrodes are placed in the torso for WCD and also for ICD, for an initial comparison. Effect of external voltage applied at the electrodes are captured through modified torso and cardiac potential generation. Efficacy of defibrillation is calculated through DFT value based on critical mass hypothesis and also extent of myocardial damage incurred. We also calculate a new efficacy measure combining DFT and myocardial damage using a probabilistic distribution and weighted Kullback Leibler (KL) divergence [24]. Schematic of the work-flow is shown in Fig.1.

A. Computational model from MRI image

MRI scan of a 19 year old healthy subject, obtained from an open source dataset [16] was used to create the geometric model. Image segmentation for cardiac section as well as different other organs and tissue in torso region was computed using an open source software Seg3D [17]. Tissue conductivity values for segmented sections were defined as per standard literature [18]. Segmented section and their conductivity values were: bowel gas, 0.002; connective tissue, 0.220; liver, 0.150; kidney, 0.070; skeletal muscle, 0.250; fat, 0.050; bone, 0.006; lung, 0.067; blood, 0.700; and myocardium, 0.250 siemens/m. A look up table was created with segmentation index and corresponding conductivity values.

WCD specifications for modeling were incorporated from 'LifeVest WCD' (Zoll Lifecor Corp.) [19]. The 'shock' electrode configuration for both ICD and WCD around the torso is shown in Fig.2. SCIRun software was used to incorporate electrode configuration on the geometric torso cardiac model. Electrodes in ICD simulation represents standard 'Can' and 'Wire'configuration [20]. 'Can' electrode was placed above the heart along mid sternal line and acted as the anode. 'Wire' electrode of 0.08 meter(m) length and 0.003 m width was configured as cathode. Defibrillation electrodes for WCD were all of similar shape and size (0.1 m $\times$ 0.1 m). For the standard three electrode configuration, 'apex' electrode acting as anode was positioned at midaxillary line at the level of the 5th intercostal space. Cathode electrodes were placed under the left and right clavicle at the 4th intercostal level. For side configuration, both anode and cathode were placed adjacent to the sternum across the mid axilliary line. Anode electrode was placed on left precordium, infront of chest and cathode was placed on the back behind the heart in between the scapulas for the front-back configuration.

B. Biophysical simulation

The steady state electrical potential in a homogeneous volume conductor is defined as $\nabla \cdot (\sigma \nabla \phi) = 0$, where, σ is the conductivity tensor field and ϕ is the electric potential [21]. Dirichlet boundary condition is applied where electric potential is known, expressed as $\phi(x,y,z) \mid_{\Omega_k} = V_k$, where V_k is the known potential of electrode k, and Ω_k specifies the domain coincident with electrode k. Neuman boundary is applied on areas of boundary not defined by Ω, expressed as $\frac{\partial \phi}{\partial n} \mid_{\Omega} = 0$.

In defined geometry, this problem can be solved via analytical expansions. However in complex geometries such as realistic torso models, numerical solutions like Finite Element Method (FEM) must be applied. FEM begins by subdividing the geometry into a set of volume elements with vertices at a set of nodes, and then approximating the potential in the volume by a basis expansion: $\bar{\phi}(x,y,z) = \sum \phi_i N_i(x,y,z)$ where N_i are a set of basis functions, one for each node in the volume element discretization, and ϕ_i are the corresponding (unknown) coefficients at those nodes. This is solved by 'Galerkin' method [22].

Manipulation of the resulting integral equations yields: $\nabla \cdot (\sigma \nabla \sum_i \phi_i N_i) = 0$. Integrating on both side results in the 'weak PDE' form : $\int_\Omega \nabla \cdot (\sigma \nabla \sum_i \phi_i N_i) N_j dV = \int_\Omega 0.N_j dV$ and subsequent simplification results in solution:

$$\sum_i \phi_i \int_{\Omega - \bar{\Omega} - \bar{\omega}_k} \sigma \nabla N_i \nabla N_j dV = 0 \qquad (1)$$

These equations were solved in SCIRun environment. The electrode models defined over space Ω was combined in the

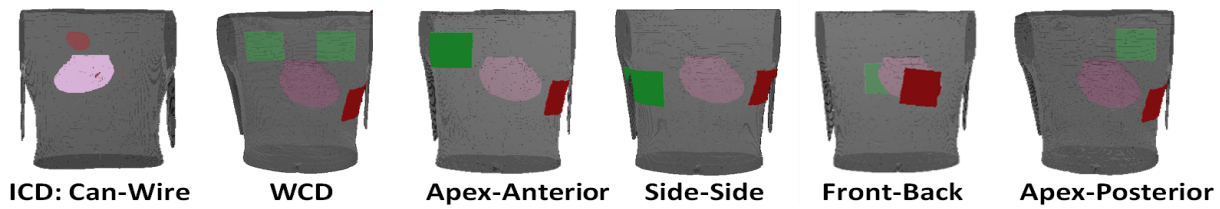

Fig. 2: Electrode configuration over the torso: ICD (posterior view), standard WCD and four custom variations (red: anode; green: cathode; anterior view)

computational mesh defined by hexahedral elements. Conductivity values for the segmented region extracted from previously created 'look up table' were projected in the mesh by sampling with linear interpolation. Potential for shock electrode (anode) was fixed at the specified values to define the strength of the applied shock, whereas potential for ground electrode (cathode) was defined to be 0 mV throughout.

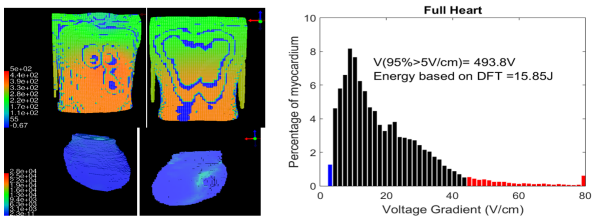

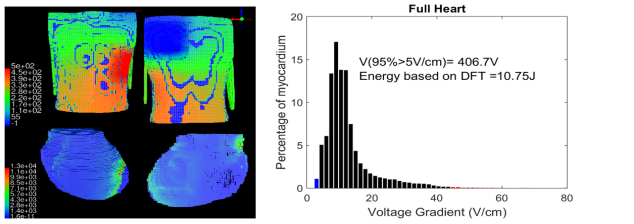

Fig. 3: Torso and Cardiac potential distribution and histogram representation of myocardium voltage gradient for modeled ICD and WCD (Apex-Anterior) response

C. Defibrillator Efficacy

The Defibrillation Threshold (DFT) is the conventional clinical metric used to define the energy or voltage required to defibrillate a patient using a particular electrotherapy. Defibrillation efficacy is assessed through 'Critical mass' theorem [14], which considers DFT value capable of changing atleast 95% myocardial mass to a potential gradient of $5V/cm$ as the effective defibrillation index. Defibrillation energy was calculated using formulation $E = \frac{1}{2}CV^2$ where $C = 130\mu F$ and V is the required DFT voltage for the particular electrode configuration [23]. DFT value reaching the critical mass is capable of stopping the VA but the shock magnitude itself has sufficient energy to damage the myocardium. We calculated the ventricular mass with a voltage gradient $> 30V/cm$ [15],$> 45V/cm$ and $> 60V/cm$, to assess possible myocardial damage.

A new measure combining DFT and myocardial damage was formulated using probabilistic distribution and weighted KL divergence (KLD). We define an ideal distribution of myocardial voltage gradient after defibrillation by combining two exponential functions, one rising and other decaying in amplitude for below and above of $5V/cm$ respectively. The distribution should be such that the required critical mass defibrillation is achieved ideally around $5V/cm$ mark and the decay component diminishes for value $>= 30V/cm$. Desired distribution is modeled as: $y = A_1 e^{\frac{-x}{\tau_1}} \quad \forall x \geqslant 5$; and $y = A_2 e^{\frac{-(5-x)}{\tau_2}} \quad \forall x < 5$; where A is the maximum amplitude, τ_1 and τ_2 are the rate constants. To preserve continuity at $x = 5V/cm$, A_2 is defined as: $A_2 = A_1 e^{\frac{-5}{\tau_1}}$. A_1 ,τ_1 and τ_2 are tuned to satisfy (i) the area under the distribution for $\leqslant 5V/cm$ and $\geqslant 5V/cm$ as 5% and 95% respectively, (ii) value of the function at $30V/cm$ is less than 2% [14]. The representative distribution is shown in blue color in Fig.5. Myocardial potential gradient distribution for different electrode configuration were compared against the modeled distribution.

Considering the modeled distribution as M and the defibrillation Voltage gradient distribution as C, the divergence or the information gain from M to C can be computed using KLD. Higher voltage gradient leads to greater myocardial damage, hence we have proposed the error measure reflecting the efficacy of the defibrillation (ED) using weighted KLD D^w_{KL} as given in eq.(2) [24]. Here the weight $(W = x)$ allows the regions with higher myocardial gradient to be penalized more in the computation of the error measure (ED). Lower the measure, lower is the difference in entropy between M and C, making the actual defibrillation function closer to the modeled or ideal one. This difference can be considered as the error between these two distributions, and provide an informative efficacy measure (ED) combining both DFT and myocardial damage information.

$$ED(C) = D^w_{KL}(C||M) = \sum_{x=0}^{\infty} x.C(x) ln \frac{C(x)}{M(x)} \qquad (2)$$

III. Result and Discussion

Defibrillation pipeline was simulated for a standard ICD defibrillation. Electrodes were placed inside torso and a uniform field of 500V was applied through the electrode to compute the effect of external field on myocardium and torso and also calculate DFT and defibrillation energy. The first figure of Fig.3 shows the shock potential distribution just after defibrillation in torso and cardiac surface. Body surface potential due to normal cardiac event hardly surpasses 5mv

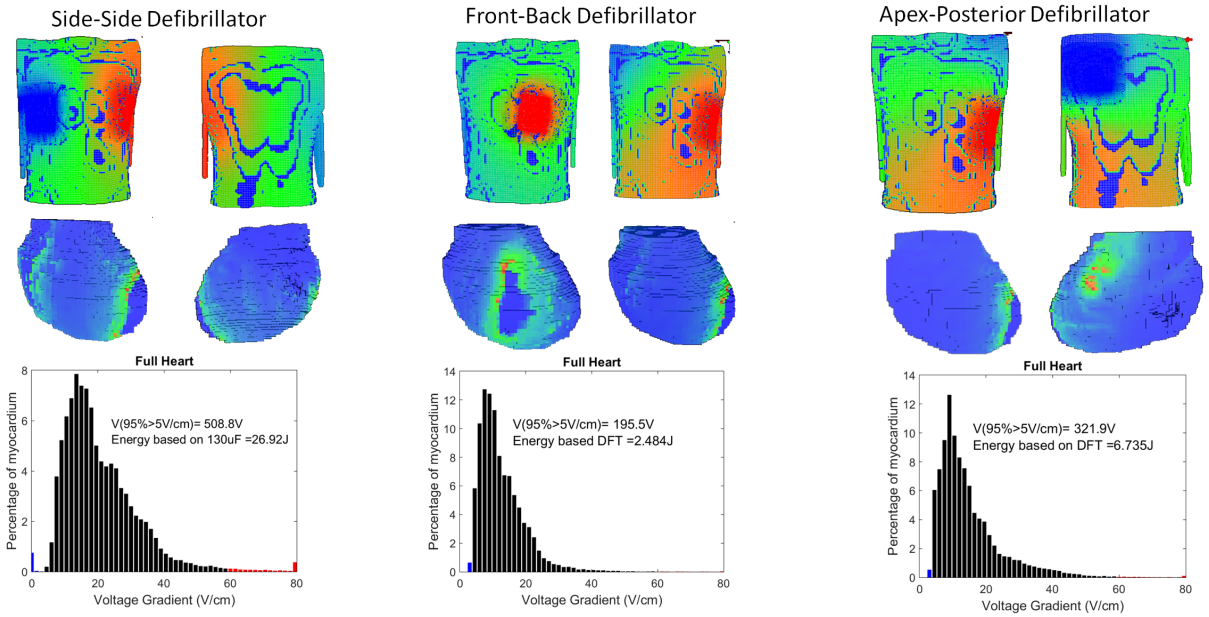

Fig. 4: Torso Cardiac potential distribution and histogram representation of myocardium voltage gradient for Side-Side, Front-Back and Apex-Posterior response

TABLE I: Defibrillator Efficacy Parameters

Config	Applied Voltage	DFT	Energy	%Myo$> 30V/cm$	%Myo$> 45V/cm$	% Myo $> 60V/cm$	ED using KLD	ED using wtdKLD
ICD	500V	493.8V	15.85J	18.035%	4.765%	1.852%	-	-
Apex-Anterior	500V	406.7V	10.75J	7.923%	1.608%	0.4348%	0.316	5.169
Side-Side	800V	508.8V	26.92J	16.97%	3.54%	1.215%	1.130	32.25
Front-Back	500V	195.5V	2.484J	2.417%	0.434%	0.142%	0.244	4.855
Apex-Posterior	500V	321.9V	6.75J	12.351%	1.608%	0.90%	0.367	11.09

range, whereas during defibrillation due to the strong external voltage, cardiac potential reaches extreme depolarized state, halting the normal rhythmic propagation and resetting the myocardial potential. DFT histogram shows the percentage distribution of myocardium against the voltage gradient. As per critical mass hypothesis, the calculated DFT reaches 95% myocardium volume over $5V/cm$ requirement, guaranteeing proper defibrillation. However, there is a considerate amount of myocardium volume exposed to a dangerously high voltage gradient ($> 45V/cm$, shown in red in Fig.3) which is sufficient for damaging those area permanently. A major application of WCD is for patients who are awaiting ICD implantation. Primary objective there is to replicate ICD credentials. The second figure in Fig.3 shows the shock potential distribution for the standard 3 electrode WCD configuration (Apex-Anterior) along with the DFT histogram. The defibrillation threshold along with the energy levels are comparable, indicating the effectiveness of the simulation pipeline in analyzing WCD behavior. It is interesting to note that WCD achieves successful defibrillation with lower defibrillation energy and also the percentage of myocardial volume in higher voltage gradient zone is lower compared to standard ICD.

We compared four standard shocking electrode configuration for WCD to analyze the effect of electrode location in Defibrillation parameter. The standard electrode configuration for 'Zoll WCD' uses two posterior shocking electrode with one apex electrode. Shock generation is through one of the posterior and the apex electrode. Other electrode configuration tested are: apex-anterior, side-side, front back and apex posterior (Fig.2). Defibrillation property of Apex-anterior configuration actually matches the standard 3 electrode configuration of WCD. Torso potential distribution reflects the external electrode field but it is interesting to note the cardiac potential distribution. For different configuration, there are certain specific regions in myocardium that reaches very high depolarized states, as shown in Fig.3 and Fig.4.

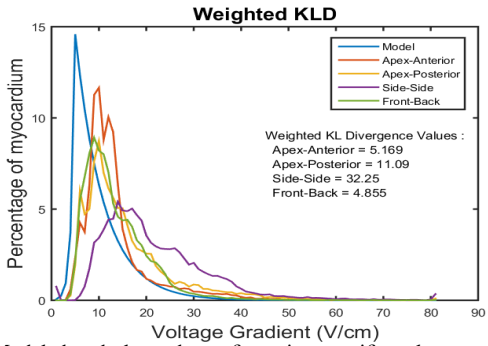

Fig. 5: Modeled and electrode configuration specific voltage gradient distribution weighted KL method

Table I compares all the defibrillator parameters for ICD and WCD configurations. Fig.5 shows the ideal (Model) potential gradient distribution ($A_1 = 0.3357$, $\tau_1 = 6, \tau_2 = 0.73$, plotted in percentage scale) along with distribution for the four different WCD configuration and the associated ED error. It is evident from the DFT value, defibrillation energy and ED error measure, that different electrode configurations result in substantially different DFTs for a particular torso. Side-side configuration of electrode is generally the most convenient location to fit in defibrillator vests, however, analysis shows that this particular configuration has the maximum voltage requirement, highest DFT and energy requirement among the other configurations and a greater possibility of myocardium damage. Between ED error using KL and weighted KL, due to the variable scaling of the distribution, configurations that has higher myocardial damage are penalized more heavily, thus generating a large error value. As indicated from the table, front-back configuration provides the best result, both in terms of DFT energy and myocardial damage index followed by apex-posterior configuration.

The FE analysis with changeable electrode configuration provided an understanding on the defibrillator efficacy parameter variation with change in shocking configuration. In similar line, the ICD potential gradient can also be optimized by varying electrode size and location. Location of the electrodes in apex and posterior or anterior section may also vary, varying the defibrillator parameters. This is particularly true for obese patient or pediatric users where use of standard configuration may provide successful defibrillation but at the cost of higher myocardial damage. Although simulation is based on a single subject data, this model provides a general pipeline that can be used for subject specific analysis and provide personalized WCD vest as per the anatomy of the patient. Data for multiple subject with varying torso geometry would help to consolidate the use-case.

IV. Conclusion

Cardiac defibrillators are lifesaving therapeutic device with potentially harming capacity if not tuned properly. With the growing demand of WCD, creation of a personalized energy distribution model based on patient's anatomy, rather than a 'one size fits all' approach, is the need of the hour. Our proposed model compares the efficiency of standard and non-standard WCD electrode placement in the torso vest, demonstrating significant differences in defibrillation efficacy associated with different strategies. A new measure is presented for performing such a comparison which combines the DFT and extend of myocardial damage. Proposed approach of tuning defibrillation parameter can also be coupled to a physical cardiac model [25]. This would enable therapeutic device validation, combining VA detection along with the proposed optimized tuning strategy.

References

[1] T. Smith, M. Cain. Sudden cardiac death: epidemiologic and financial worldwide perspective. J Interv Card Electrophysiol, vol: 17, pp:199-203, 2006.

[2] G. Nichol, M. Sayre, F. Guerra, J. Poole, Defibrillation for Ventricular Fibrillation: A Shocking Update, Journal of the American College of Cardiology, vol:70(12), 2017.

[3] J. Groot, Why shocking might be not shocking enough, Cardiovascular Research, Vol:61, pp: 9-10, 2004.

[4] J. Poole, G. Johnson, A. Hellkamp, J. Anderson, D. Callans, M. Raitt. Prognostic importance of defibrillator shocks in patients with heart failure. N Engl J Med, vol:359, pp:1009-1017, 2008.

[5] J. Barraud, J. Cautela, M. Orabona, O. Missenard, M. Laine, F. Thuny, F. Paganelli, L. Bonello, M. Peyrol, Wearable cardioverter defibrillator: Bridge or alternative to implantation?, World J Cardiol, vol: 9(6): 531-538, 2017.

[6] P. Sharma, P. Bordachar, and K. Ellenbogen; Indications and use of the wearable cardiac defibrillator, European Heart Journal, vol:38, pp:258-267, 2107.

[7] C. Wan, W. Jess, O. Steven, J. Szymkiewicz, Successful Use of Wearable Cardioverter Defibrillator in a Patient with Dextrocardia and Persistent Left Superior Vena Cava; Ann Noninvasive Electrocardiol; vol:18(5),pp: 487-490, 2013.

[8] A. Epstein, W. Abraham, N. Bianco, K. Kern, S. Rao, E. Rhee, S.Solomon, S. Szymkiewicz, Wearable Cardioverter-Defibrillator Use in Patients Perceived to be at High Risk Early Post-Myocardial Infarction,Journal of the American College of Cardiology; vol:62(21), 2013.

[9] A. Colley, S. Williams, K. Rhode, C. Rinaldi, M. Bishop; Conceptual intra-cardiac electrode configurations that facilitate directional cardiac stimulation for optimal electrotherapy, IEEE Trans Biomed Eng. vol:66(5), pp: 1259-1268, 2019 doi:10.1109/TBME.2018.2871863.

[10] N. Trayanova, J. Constantino and G. Plank, Modeling Defibrillation of the Heart: Approaches and Insights, ,IEEE Rev Biomed Eng, vol:4, pp: 89-102, 2011.

[11] D. Dosdall, V. Fast, and Raymond E. Ideker, Mechanisms of Defibrillation Annu Rev Biomed Eng. vol: 12, pp: 233-258, 2010.

[12] L. Qiana, J. Wanga, L. Jina, B. Songa and X. Wua, Effect of ventricular myocardium characteristics on the defibrillation threshold, Technology and Health Care; IOS Press, vol: 26, 2018.

[13] A. Onofrio, V. Russo, V. Bianchi, C. Cavallaro, S. Leonardi, P. Mocavero, and G. Nigro; Effects of defibrillation shock in patients implanted with a subcutaneous defibrillator: a biomarker study, Europace, vol: 20, pp:233-239, 2018.

[14] D. Zipes, J. Fischer, R. King, A. Nicoll, W. Jolly, Termination of ventricular fibrillation in dogs by depolarizing a critical amount of myocardium. Am J Cardiol; vol:36, pp: 37-44, 1975.

[15] J. Stinstra, J. Tat, S. Pieper, R. MacLeod, L. Chu L, P.Wang, J. Triedman, Finite element modeling of subcutaneous implantable defibrillator electrodes in an adult torso., Heart Rhythm. J; vol: 7(5); pp:692-698, 2010

[16] http://www.scirun.org; SCIRun: A Scientific Computing Problem Solving Environment, Scientific Computing and Imaging Institute (SCI),2016

[17] www.sci.utah.edu/cibc-software/seg3d

[18] S. Morgan, G. Plank, V. Irina, and N. Vadim,Low Energy Defibrillation in Human Cardiac Tissue: A Simulation Study, Biophysical Journal, vol:96, pp:1364-1373, 2009.

[19] S. Reek, H. Burri, P. Roberts, C. Perings, A. Epstein, and H. Klein, The wearable cardioverter-defibrillator: current technology and evolving indications, Europace vol:19, pp: 335-345, 2017.

[20] J. Stinstra, S. Pieper, R. MacLeod, D. Brooks, F. Cecchin, J. Triedman, A computer modeling tool for comparing novel ICD electrode orientations in children and adults, Heart Rhythm. J, vol:5(4), pp:565-572, 2008.

[21] J. Stinstra, M. Jolley, M. Callahan, Evaluation of different meshing algorithms in the computation of defibrillation thresholds in children. Conf Proc IEEE Eng Med Biol Soc, pp:1422-1425, 2017.

[22] H. Lim, W. Cun, Y. Wang, R. Gray, and J. Glimm, The role of conductivity discontinuities in design of cardiac defibrillation, Chaos, vol: 28, 2018.

[23] H. Karagueuzian, P. Chen, Cellular mechanism of reentry induced by a strong electrical stimulus: Implications for fibrillation and defibrillation, Cardiovascular Research, vol:50, pp: 251-262, 2001.

[24] Y. Sekeh, S. Borzadaran, G. Reza, Abdolhamid, On Kullback-Leibler Dynamic Information, Journal available at SSRN 2344078, 2013.

[25] O. Mazumder, D. Roy, S. Bhattacharya, A. Sinha, and A. Pal, Synthetic ppg generation from hemodynamic model with baroreflex autoregulation: a digital twin of cardiovascular system, in 2019 41th Annual International Conference of the IEEE Engineering in Medicine and Biology Society (EMBC). IEEE, 2019, pp. 5489-5492.